# Whole-body biomechanical load in running-based sports

Verheul, J.; Gregson, Warren; Lisboa, Paulo; Vanrenterghem, Jos; Robinson, Mark A.

*DOI:*
10.1016/j.jsams.2018.12.007

# Whole-body biomechanical load in running-based sports: the validity of estimating ground reaction forces from segmental accelerations

**Original research article**

**Authors**:

Jasper Verheul[1], Warren Gregson[1], Paulo Lisboa[2], Jos Vanrenterghem[3], Mark A. Robinson[1]

1. Research Institute for Sport and Exercise Sciences, Liverpool John Moores University, Liverpool, United Kingdom
2. Department of Applied Mathematics, Liverpool John Moores University, Liverpool, United Kingdom
3. Faculty of Kinesiology and Rehabilitation Sciences, KU Leuven, Leuven, Belgium

**Corresponding Author**:

Jasper Verheul (J.P.Verheul@2016.ljmu.ac.uk)

Research Institute for Sport and Exercise Sciences, Liverpool John Moores University

Tom Reilly Building, Byrom Street, L3 5AF, Liverpool, United Kingdom

**Abstract word count**: 250

**Text-only word count**: 3519

**Number of figures and tables**: 2 figures and 1 table

# Whole-body biomechanical load in running-based sports: the validity of estimating ground reaction forces from segmental accelerations


## Abstract

*Objective:* Unlike physiological loads, the biomechanical loads of training in running-based sports are still largely unexplored. This study, therefore, aimed to assess the validity of estimating ground reaction forces (GRF), as a measure of external whole-body biomechanical loading, from segmental accelerations.

*Methods:* Fifteen team-sport athletes performed accelerations, decelerations, 90° cuts and straight running at different speeds including sprinting. Full-body kinematics and GRF were recorded with a three-dimensional motion capture system and a single force platform respectively. GRF profiles were estimated as the sum of the product of all fifteen segmental masses and accelerations, or a reduced number of segments.

*Results*: Errors for GRF profiles estimated from fifteen segmental accelerations were low (1-2 $N \cdot kg^{-1}$) for low-speed running, moderate (2-3 $N \cdot kg^{-1}$) for accelerations, 90° cuts and moderate-speed running, but very high (>4 $N \cdot kg^{-1}$) for decelerations and high-speed running. Similarly, impulse (2.3-11.1%), impact peak (9.2-28.5%) and loading rate (20.1-42.8%) errors varied across tasks. Moreover, mean errors increased from $3.26 \pm 1.72\ N \cdot kg^{-1}$ to $6.76 \pm 3.62\ N \cdot kg^{-1}$ across tasks when the number of segments was reduced.

*Conclusions:* Accuracy of estimated GRF profiles and loading characteristics was dependent on task, and errors substantially increased when the number of segments was reduced. Using a direct mechanical approach to estimate GRF from segmental accelerations is thus unlikely to be a valid method to assess whole-body biomechanical loading across different dynamic and high-intensity activities. Researchers and practitioners should, therefore, be very cautious when interpreting accelerations from one or several segments, as these are unlikely to accurately represent external whole-body biomechanical loads.

**Keywords**: Training load monitoring; Biomechanical loads; Full-body segmental accelerations; Loading characteristics; Segment reductions

**Introduction**

Training loads are monitored in sports as part of a process which aims to enhance performance, whilst simultaneously reducing the risk of injury. Although physiological loads have been investigated extensively, biomechanical load measures are still limited and, therefore, largely unexplored [1]. Based on the assumption that accelerations of the trunk are a good representation of whole-body centre of mass (CoM) accelerations, trunk accelerometry derived load measures (e.g. New Body Load, Dynamic Stress Load, PlayerLoad, Force Load) have been used to quantify and evaluate whole-body biomechanical loads [2–6]. However, evidence relating accelerations of the trunk to established measures of biomechanical loading is yet lacking. In fact, it has been shown that accelerations of individual segments (including the trunk) cannot accurately represent whole-body biomechanical loads [7–11].

Ground reaction forces (GRFs) are a well-established measure of whole-body biomechanical loading. GRFs have been used to optimise sprint performance [12,13], improve running economy [14] and identify or reduce potential injury risk factors [15,16], and might thus be used to further understand the role of external biomechanical forces in performance enhancement and injury prevention. Moreover, GRF drives internal force production and contributes to internal stresses on e.g. muscles, tendons and bones [17,18], which are currently difficult to measure in the field [1]. Since these structure- or tissue-specific loads are the primary cause of e.g. overuse injuries [19], monitoring GRF in the field would be a first step towards investigating internal biomechanical loads in more detail. However, valid methods for accurately estimating GRF outside laboratory settings are currently unavailable.

Body-worn sensors, such as accelerometers, are commonly used in sports to measure and monitor numerous training load related metrics [20,21]. Given their widespread application to measure accelerations of various body segments [22,23], accelerometers might be used to estimate GRF, which can be defined as the sum of the product of segmental mass and CoM accelerations of all body segments. This alternative expression of Newton's second law provides a way by which the contribution of multiple segmental accelerations to the GRF can be systematically examined, especially since accelerations of the trunk or other individual segments have been shown to not be sufficient to estimate GRF for several straight running and cutting activities [7–9,11,24]. Other studies have indeed shown that for constant speed running, GRF can be estimated from seven [25] or eleven [26] segmental accelerations measured with a laboratory based motion capture system. However, it is unknown whether GRF for dynamic and high-intensity activities frequently undertaken in running-based sports (e.g. rapidly accelerating, decelerating, cutting, sprinting) can be accurately estimated from segmental accelerations and/or what the minimal required number of segments is.

If simultaneously measured segmental accelerations can be used to estimate GRF, this might eventually allow GRF to be estimated in field settings and provide a meaningful measure of external whole-body biomechanical loading. The aim of this study was, therefore, 1) to investigate whether segmental accelerations measured in a laboratory setting can be used to estimate GRF for a variety of dynamic and high-intensity tasks typically performed during running-based (team-) sports, and 2) to determine the minimal number of segments required.

**Methods**

*Participants*. Fifteen team-sports athletes participated in this study (12 males and 3 females, age 23±4 yrs, height 178±9 cm, body mass 73±10 kg). All participants were healthy and physically active for at least three hours per week (sports participation 7±5 hrs per wk). This study was approved by the Liverpool John Moores University ethics committee and participants provided informed consent according to the ethics regulations.

*Protocol*. After a standardised warm-up, participants performed a range of dynamic and high-intensity running tasks including accelerations, decelerations, cutting, and steady running at constant speeds ranging from 2 $m \cdot s^{-1}$ to maximal sprinting (~7 $m \cdot s^{-1}$, individual specific). Participants were instructed to land with one whole foot on a single force platform embedded in the ground and performed a minimum of five trials for each leg per task. For acceleration trials, participants were instructed to accelerate from stand-still to their maximal sprinting speed (achieved in ~20 m), while landing on the force platform for their second or third step of accelerating. For decelerations, participants were instructed to decelerate as quickly as possible from maximal sprinting to immediate stand-still, while landing on the force platform for their first or second step of decelerating. Cutting trials were performed as a sharp change of direction on the force platform at a 90° angle from the straight running direction. Steady (straight) running trials were performed at a constant low (2-3 m·s$^{-1}$), moderate (4-5 m·s$^{-1}$) or high running speed (>6 m·s$^{-1}$), including maximal sprinting. Running speeds were measured with photocell timing gates (Brower Timing Systems, Draper, UT, USA) and controlled by giving verbal feedback to speed up or slow down after each trial. Only trials within a ± 5% range of the target speed were included.

*Kinematic and kinetic data collection*. During the trials, full-body kinematic data were collected using a seventy-six retro-reflective marker set attached to anatomical landmarks of the body (appendix A). Three-dimensional kinematic and kinetic data were synchronously recorded with ten infrared cameras (Qqus 300+, Qualisys Inc., Gothenburg, Sweden) sampling at 250 Hz, in combination with a single force platform (9287B, 90x60 cm, Kistler Holding AG, Winterthur, Switzerland) embedded in the ground, sampling at 3000 Hz. Marker positions and ground reaction forces (GRF) were recorded, synchronised and tracked using Qualisys Track Manager Software (QTM version 2.16, Qualisys Inc., Gothenberg, Sweden). A static calibration was recorded at the start of each session to determine the local coordinate systems, joint centres and segment dimensions for each participant. From the marker data, a fifteen segment (head, trunk, pelvis, upper arms, forearms, hands, thighs, shanks and feet) six-degree-of-freedom model was built, with segment mass and inertial properties based on Dempster's regression equations [27] and represented as geometric volumes [28]. Kinematic and kinetic data were exported to Visual3D (C-motion, Germantown, MD, USA) and Matlab (version R2017b, The MathWorks, Inc., Natick, MA, USA) for further processing and analysis.

*Data processing and analysis*. Marker trajectories and force platform data were filtered with a 2$^{nd}$ order Butterworth low-pass filter with 20 Hz and 50 Hz cut-off frequencies respectively. Trunk defining marker trajectories were, however, filtered at 10 Hz based on a sensitivity analysis for optimal GRF prediction (appendix B). For each trial, touch-down and take-off from the force platform were identified by a 20 N threshold of the vertical GRF and resultant GRF was calculated from the three individual force components ($F_x$, $F_y$, $F_z$). The centre of mass (CoM) position for each segment was used to define segmental movements from which accelerations were calculated as the double differentiation (using three-point derivatives) of CoM motion along the three axes of the lab (x-y-z). Resultant GRF curves were then estimated as the sum of the product of each segmental mass and CoM acceleration in the three directions, according to equation 1.

$$\mathrm{GRF}_{\mathrm{res,estimated}} = \sqrt{\left(\sum_{n=1}^{1,2,3,\ldots 15}\left(a_{n,x}\cdot m_n\right)\right)^2+\left(\sum_{n=1}^{1,2,3,\ldots 15}\left(a_{n,y}\cdot m_n\right)\right)^2+\left(\sum_{n=1}^{1,2,3,\ldots 15}\left(a_{n,z}\cdot m_n\right)\right)^2} \qquad \text{Eq. 1}$$

In which *a* is the segmental acceleration, *m* the segmental mass and *n* the number of segments included. To determine the number of segments required to accurately estimate resultant GRF, all different segment combinations to estimate GRF from were examined. A total of 32,676 unique combinations were analysed with a minimum of one and a maximum of fifteen segments. To ensure a constant total body mass, masses of the segments not included in a specific combination were equally divided and added to the segmental masses that were part of that combination.

Measured and estimated GRF curves were normalised to each participant's body mass. Accuracy of estimated GRF profiles was evaluated by the absolute and relative curve root mean square errors (RMSE). In addition, the accuracy of estimated GRF loading characteristics impulse (area under the GRF curve), impact peak (force peak during the first 30% of stance) and loading rate (average GRF gradient from touch-down to impact peak) was calculated and assessed. RMSE was rated as very low ($<1\ \mathrm{N\cdot kg^{-1}}$), low ($1\text{-}2\ \mathrm{N\cdot kg^{-1}}$), moderate ($2\text{-}3\ \mathrm{N\cdot kg^{-1}}$), high ($3\text{-}4\ \mathrm{N\cdot kg^{-1}}$) or very high ($>4\ \mathrm{N\cdot kg^{-1}}$). RMSE values were analysed for all possible combinations of segments per task, as well as all trials combined, to determine the best combination (i.e. lowest mean RMSE across trials) for each number of segments. Estimated GRF loading characteristics errors were rated as very low (<5%), low (5-10%), moderate (10-15%), high (15-20%) or very high (>20%), which was based on meaningful performance or injury related differences in GRF [12,13,15]. Moreover, linear regression analyses were performed between GRF loading characteristics (impulse, impact peak, loading rate) derived from the estimated and measured GRF profiles. Regressions were performed per task, as well as for all trials combined to examine the generalisability of GRF estimations across tasks, and rated as very weak ($R^2<0.1$), weak ($R^2=0.1\text{-}0.3$), moderate ($R^2=0.3\text{-}0.5$), strong ($R^2=0.5\text{-}0.7$), very strong ($R^2=0.7\text{-}0.9$) or extremely strong ($R^2=0.9\text{-}1$) [29]. Furthermore, Bland-Altman analyses [30] were performed across tasks to explore mean differences and 95% limits of agreement between the estimated and measured GRF loading characteristics.

## Results

*Full body segmental accelerations*. Accuracy of estimated GRF profiles from fifteen segmental accelerations (full-body) varied across tasks (figure 1; table 1). Overall curve errors (RMSE) were low for running at low speeds (2-3 $m{\cdot}s^{-1}$) and moderate for accelerations, 90° cuts and moderate-speed (4-5 $m{\cdot}s^{-1}$) running. However, mean RMSE was very high for decelerations and high-speed running (>6 $m{\cdot}s^{-1}$).

The accuracy of estimated GRF loading characteristics varied between metrics and was dependent on task (table 1). Impulses were accurately estimated with very low errors for 90° cuts and running at constant low and moderate speeds, low errors for accelerations, and moderate errors for decelerations and high-speed running. Similarly, impact peaks were estimated with low to moderate (9.2-15%) errors for all tasks, except accelerations, which had very high (28.5%) impact peak errors. Loading rate errors however, were very high (20.1-42.8%) across all tasks.

Correlations and agreement between measured and estimated GRF loading characteristics across all tasks varied. Impulses had extremely strong correlations, with a small bias and 95% confidence interval of the limits of agreement (-0.04 to 0.45 $N{\cdot}s{\cdot}kg^{-1}$) (figure C.1 A and D; table 1). Despite the very strong correlation and small bias for impact peaks however, there was a large variation of the differences with limits of agreement ranging from -12.6 to 8.4 $N{\cdot}kg^{-1}$ (figure C.1 B and E). Furthermore, measured and estimated loading rates had a strong correlation ($R^2 = 0.68$), but a large bias and limits of agreement (-985 to 397 $N{\cdot}kg^{-1}{\cdot}s^{-1}$) (figure C.1 C and F).

*Segment reductions*. The best combinations of segments across all tasks for each given number of segments are shown in table C.1. GRF estimated from a single segment was the best across tasks from trunk accelerations, despite mean RMSE being very high. Furthermore, the trunk was part of all combinations of segments, and thus the main contributor to GRF, followed by the thighs, head, shanks, arms, pelvis and feet (in descending order of importance).

Reducing the number of segmental accelerations to estimate GRF substantially increased errors for all tasks (figure 2). To achieve estimated GRF errors that were moderate or better (<3 N·kg$^{-1}$) for at least 50% of the combinations and trials, a minimum of two and three segments was required for low- and moderate-speed running respectively, but eight (90° cuts) and eleven (accelerations) for more dynamic tasks. Moreover, for the high-intensity tasks (decelerations and high-speed running) the majority of trials and combinations resulted in very high errors, regardless of the number of segment used (figure 2).

## Discussion

*Estimating GRF from full-body segmental accelerations*. The main aim of this study was to assess the validity of estimating ground reaction forces (GRF) from segmental accelerations for a range of dynamic and high-intensity running tasks typically performed during running-based sports. From all fifteen body segments, overall GRF profiles as well as specific loading characteristics were estimated with varying accuracy. Overall loading errors (RMSE and impulse) for example, were considerably lower for running at low and moderate speeds (~2-5%) compared to the higher intensity tasks (e.g. decelerations, high-speed running) (~6-12%). Similarly, impact peak and loading rate errors ranged from ~9% for the lower intensity tasks to >40% for higher intensity tasks (figure C.1 E and F). Meaningful performance or injury related differences in loading characteristics can, however, be as small as ~3-10% [12,13,15]. Errors of the magnitude observed in this study could thus already rule out certain applications of monitoring GRF estimated from full-body segmental accelerations. Using a direct mechanical approach to estimate GRF from full-body segmental accelerations might, therefore, not be a valid method to assess whole-body biomechanical loading for dynamic and high-intensity activities. Consequently, future research should investigate if segmental accelerations might be used to assess more specific measures of biomechanical loading (e.g. internal structural loads).

Estimated GRF results in this study are comparable to other laboratory-based studies aiming to predict GRF from marker trajectory data using a mechanical approach. The impulse errors for low-speed running (2.3%), impact peak errors for moderate-speed running (9.2%) and correlations between estimated and measured impact peaks for low- to high-speed running ($R^2$=0.77-0.96) found in the current study are similar to results reported in previous studies that aimed to predict GRF from marker trajectory data for comparable constant speed running tasks [25,26,31]. However, this study extends beyond other studies in that similar results were also achieved for a range of high-intensity and dynamic running tasks frequently undertaken in running-based sports. Moreover, previous studies failed to include the mediolateral and anteroposterior components of acceleration and GRF [25,31], utilised small sample sizes [25,26,31] and/or investigated running on a treadmill rather than overground [26,31], all of which limit their ability to translate their findings from the lab to an applied sport setting.

In most running-based sports, the dynamic and high-intensity movements examined in this study are regularly performed [32–34]. The musculoskeletal demands of these tasks are high [35–37] and thus comprise a large amount of the total biomechanical loads experienced during training and competition. Therefore, highly accurate estimates of GRF loading characteristics across different tasks (including decelerations and running at high speeds) are essential to explore and understand the biomechanical demands of training in greater detail. As discussed above however, the loading characteristics errors observed in this study might already rule out several performance and injury related applications of monitoring GRF. Future work could, therefore, investigate if the strong to extremely strong correlations between estimated and measured GRF characteristics found in this study (figure C1; table 1) can be used to recalculate and improve the estimated loading characteristics, to quantify the biomechanical stresses of training more accurately.

*Segment reductions*. Full-body wireless accelerometry suits have been shown to be a reliable and valid method for simultaneously measuring accelerations of all body segments (e.g. Xsens MVN [38]) and have been used to estimate GRF and moments during walking [39]. It is, however, likely to be unpractical to use these systems for load monitoring during training and competition on a day-to-day basis. Therefore, we examined the effects of reducing the number of segments and the minimal number of segments required for acceptable GRF estimates. Although the lower intensity tasks (low- and moderate-speed running) were relatively robust against segment reductions, estimated GRF profiles for the more sport-specific dynamic and high-intensity tasks substantially deteriorated (figure 2). When the number of segmental accelerations was reduced to six segments for instance (i.e.

excluding the head, arms and feet), errors substantially increased to very high for all tasks (figure 2; table C.1). Previous studies have reported similar findings of considerably decreased accuracy in whole-body CoM estimates (and thus GRF) for constant speed running [7], side cutting [11], and jumping, kicking and throwing [40], when the number of segments was only slightly reduced. Furthermore, the very high errors observed in this study for GRF estimated from one segment (i.e. the trunk) are in line with other studies which reported that individual segmental accelerations cannot be used to accurately estimate GRF for steady running at constant speeds [7,9] and side cutting [8,11]. These findings, together with the present results suggest that estimating GRF from one or several segmental accelerations using a mechanical approach is not a valid method to accurately predict GRF for dynamic and high-intensity running tasks.

A crucial requirement for GRF to be used as a meaningful measure of biomechanical loading in the field, is that GRF estimates are highly accurate across different tasks. Since errors of the magnitude observed in this study might already rule out certain applications as discussed above, the increased GRF errors for a reduced number of segments probably further eliminate several aspects that make GRF a meaningful load measure. Consequently, the usefulness of less accurate GRF estimates from a reduced number of segments (and individual segmental accelerations from e.g. the trunk especially) as a measure of biomechanical loading, is questionable. Researchers and practitioners should, therefore, be very cautious when interpreting one or several segmental accelerations (or derived load measures), as these are unlikely to be a valid and meaningful measure of whole-body biomechanical loading.

*Alternative methods to assess whole-body biomechanical loading in the field.* Segmental accelerations used to estimate GRF in this study were derived from marker trajectory data recorded with a three-dimensional motion capture system. Similar to force platforms, such systems are not typically available in the field and if they are, data collection is laborious and impractical for immediate analysis on a daily basis. In contrast to force platform and marker-based motion capture technologies however, body-worn accelerometers are commonly used in the field and thus relatively easily accessible [20,21]. Moreover, the use of in-field markerless motion capture systems are currently on the rise as a non-invasive way of quantifying movement in different sports [41–43]. Future research should, therefore, investigate if body-worn (or even implantable [44]) accelerometers or markerless motion capture systems can provide accurate measures of full-body segmental CoM accelerations, to eventually estimate GRF in field settings.

This study aimed to estimate GRF from segmental accelerations using a direct mechanical approach. Alternative methods have, however, emerged that use machine learning methods to predict GRF [45–48]. For example, neural network approaches have been used successfully to predict GRF from marker trajectory data [46,48] or body-worn accelerometers [45,47] for a variety of running tasks. Despite the promising results, there might be disadvantages of using these computational rather than mechanical approaches to estimate GRF for load monitoring purposes. Computational methods could prevent one from exploring the underlying physical mechanisms of the predicted variable (e.g. GRF, joint moments) which may limit its use for e.g. explaining injury mechanisms or defining performance enhancing criteria. Machine learning could thus offer a powerful alternative for our mechanistic approach, but future research should examine the explanatory ability of these methods for underlying physical mechanisms.

*Methodological limitations.* A limitation of the mechanical approach described in this study is that estimated GRF errors are solely due to measurement and methodological inaccuracies. Segmental masses and inertial properties for example, were based on standardised values relative to the total body mass [27] and standardised geometric shapes [28] respectively. Future work could, therefore, investigate how the present results might be improved by using participant-specific properties measured from e.g. a DXA scanner [49,50]. Other factors that could affect the estimated GRF accuracy are soft-tissue artefacts [51] and filter cut-off frequencies [52,53]. For example, impact peak errors increased for higher magnitudes, especially for decelerations (figure 2; table 1). These increased errors are likely due to the considerably higher impacts, and consequent tissue vibrations, of landing for these higher-intensity tasks. A sensitivity analysis of different cut-off filters showed that applying a lower 10 Hz filter to the trunk marker (which typically were more affected due to their attachment to tight-fitting clothing rather than the skin) resulted in the lowest estimated GRF errors across the different tasks (appendix B). Future work should, however, consider the effects of soft-tissue artefact and filter cut-off frequency, as well as the use of different filters for kinematic and kinetic data, when estimating GRF from segmental accelerations.

## Conclusions

This study showed that accuracy of GRF profiles and loading characteristics estimated from full-body segmental accelerations is dependent on task. Moreover, errors substantially increased when the number of segments was reduced. It is, therefore, unlikely that one or several segmental accelerations can provide valid estimates of GRF for biomechanical load monitoring purposes, using a direct mechanical approach. Researchers and practitioners should, therefore, be very cautious when interpreting accelerations from one or several segments as these are unlikely to accurately represent external whole-body biomechanical loads.

## Practical applications

- We suggest ground reaction forces (GRF) as a meaningful measure of overall whole-body biomechanical loading, and a first step towards investigating structure-specific internal loads, in running-based sports.
- Accuracy of GRF profiles and loading characteristics estimated from fifteen segmental accelerations was dependent on task, with higher accuracy for lower intensity tasks (e.g. running at low speeds). Moreover, errors substantially increased when the number of segments was reduced.
- A direct mechanical approach cannot provide valid estimates of GRF from segmental accelerations across dynamic and high-intensity running tasks that are frequently performed during running-based sports.
- Acceleration signals and derived training load measures from one or several segments are unlikely to accurately represent whole-body biomechanical loads.
- Researchers and practitioners should be very cautious when interpreting accelerations from one or several segments as a measure of external whole-body biomechanical loading.

**Acknowledgements**

This study did not receive any external financial support.

**Supplementary files**

Figure C.1 and table C.1 can be found in Appendix C. Appendices A, B and C are available as online supplementary documents.

## References

1. Vanrenterghem J, Nedergaard NJ, Robinson MA, Drust B. Training Load Monitoring in Team Sports: A Novel Framework Separating Physiological and Biomechanical Load-Adaptation Pathways. *Sport Med*. 2017. doi:10.1007/s40279-017-0714-2.

2. Boyd LJ, Ball K, Aughey RJ. The reliability of minimaxX accelerometers for measuring physical activity in australian football. *Int J Sports Physiol Perform*. 2011;6:311-321.

3. Ehrmann FE, Duncan CS, Sindhusake D, Franzsen WN, Greene DA. GPS and Injury Prevention in Professional Soccer. *J Strength Cond Res*. 2016;30(2):360-367.

4. Page RM, Marrin K, Brogden CM, Greig M. Biomechanical and physiological response to a contemporary soccer match-play simulation. *J Strength Cond Res*. 2015;29(10):2860-2866.

5. Gaudino P, Iaia FM, Strudwick AJ, et al. Factors Influencing Perception of Effort (Session-RPE) During Elite Soccer Training. *Int J Sports Physiol Perform*. 2015;10:860-864. doi:10.1123/ijspp.2014-0518.

6. Colby MJ, Dawson B, Heasman J, Rogalski B, Gabbett TJ. Accelerometer and GPS-Derived Running Loads and Injury Risk in Elite Australian Footballers. *J Strength Cond Res*. 2014;28(8):2244-2252.

7. Pavei G, Seminati E, Cazzola D, Minetti AE. On the estimation accuracy of the 3D body center of mass trajectory during human locomotion: Inverse vs. forward dynamics. *Front Physiol*. 2017;8(MAR):1-13. doi:10.3389/fphys.2017.00129.

8. Nedergaard NJ, Robinson MA, Eusterwiemann E, Drust B, Lisboa PJ, Vanrenterghem J. The relationship between whole-body external loading and body-worn accelerometry during team sports movement. *Int J Sports Physiol Perform*. 2017;12:18-26.

9. Raper DP, Witchalls J, Philips EJ, Knight E, Drew MK, Waddington G. Use of a tibial

accelerometer to measure ground reaction force in running: A reliability and validity comparison with force plates. *J Sci Med Sport*. 2018;21(1):84-88. doi:10.1016/j.jsams.2017.06.010.

10. Wundersitz DWT, Netto KJ, Aisbett B, Gastin PB. Validity of an upper-body-mounted accelerometer to measure peak vertical and resultant force during running and change-of-direction tasks. *Sport Biomech*. 2013;12(4):403-412. doi:10.1080/14763141.2013.811284.

11. Vanrenterghem J, Gormley D, Robinson M, Lees A. Solutions for representing the whole-body centre of mass in side cutting manoeuvres based on data that is typically available for lower limb kinematics. *Gait Posture*. 2010;31(4):517-521. doi:10.1016/j.gaitpost.2010.02.014.

12. Bezodis NE, North JS, Razavet JL. Alterations to the orientation of the ground reaction force vector affect sprint acceleration performance in team sports athletes. *J Sports Sci*. 2017;35(18):1817-1824. doi:10.1080/02640414.2016.1239024.

13. Hunter J, Marshall R, McNair P. Relationship between ground reaction force impluse and kinematics of sprint-running acceleration. *J Appl Biomech*. 2005;21:31-43. doi:10.1123/jab.21.1.31.

14. Moore IS. Is There an Economical Running Technique? A Review of Modifiable Biomechanical Factors Affecting Running Economy. *Sport Med*. 2016;0(0). doi:10.1007/s40279-016-0474-4.

15. Bazuelo-Ruiz B, Durá-Gil J V., Palomares N, Medina E, Llana-Belloch S. Effect of fatigue and gender on kinematics and ground reaction forces variables in recreational runners. *PeerJ*. 2018;6:e4489. doi:10.7717/peerj.4489.

16. Willy RW, Buchenic L, Rogacki K, Ackerman J, Schmidt A, Willson JD. In-field gait retraining and mobile monitoring to address running biomechanics associated with tibial stress fracture. *Scand J Med Sci Sports*. 2016;26(2):197-205. doi:10.1111/sms.12413.

17. Loundagin LL, Schmidt T, Edwards WB. Mechanical Fatigue of Bovine Cortical Bone Using Ground Reaction Force Waveforms in Running. *J Biomech Eng*. 2018;140(3):1-5. doi:10.1115/1.4038288.

18. Scott SH, Winter DA. Internal forces at chronic running injury sites. *Med Sci Sport Exerc*. 1990;22(3):357-369.

19. Edwards WB. Modeling Overuse Injuries in Sport as a Mechanical Fatigue Phenomenon. *Exerc Sport Sci Rev*. 2018;46(4):224-231. doi:10.1249/JES.0000000000000163.

20. Cardinale M, Varley MC. Wearable Training-Monitoring Technology: Applications, Challenges, and Opportunities. *Int J Sports Physiol Perform*. 2017;12(S2):55-62.

21. Camomilla V, Bergamini E, Fantozzi S, Vannozzi G. Trends Supporting the In-Field Use of Wearable Inertial Sensors for Sport Performance Evaluation: A Systematic Review. *Sensors*. 2018;18(3):873. doi:10.3390/s18030873.

22. Chambers R, Gabbett TJ, Cole MH, Beard A. The Use of Wearable Microsensors to Quantify Sport-Specific Movements. *Sport Med*. 2015;45(7):1065-1081. doi:10.1007/s40279-015-0332-9.

23. Dellaserra CL, Gao Y, Ransdell L. Use of integrated technology in team sports: a review of opportunities, challenges, and future directions for athletes. *J Strength Cond Res*. 2014;28(2):556-573. doi:10.1519/JSC.0b013e3182a952fb.

24. Nedergaard NJ, Robinson MA, Drust B, Lisboa PJ, Vanrenterghem J. Predicting ground reaction forces from trunk kinematics: a mass-spring-damper model approach. In: *35th Conference of the International Society of Biomechanics in Sports*. ; 2017:432-435.

25. Bobbert MF, Schamhardt HC, Nigg BM. Calculation of vertical ground reaction force estimates during running from positional data. *J Biomech*. 1991;24(12):1095-1105. doi:10.1016/0021-9290(91)90002-5.

26. Pavei G, Seminati E, Storniolo JLL, Peyré-Tartaruga LA. Estimates of running ground reaction force parameters from motion analysis. *J Appl Biomech*. 2017;33(1):69-75. doi:10.1123/jab.2015-0329.

27. Dempster WT. Space requirements of the seated operator: Geometrical, Kinematic, and Mechanical Aspects of the Body With Special Reference to the Limbs. *WADC Tech Rep*. 1955:55-159.

28. Hanavan EP. A mathematical model of the human body. *WADC Tech Rep AMRL-TR-64-102, Aerosp Med Researsch Lab Wright-Patterson Air Force Base, OH*. 1964.

29. Hopkins WG, Marshall SW, Batterham AM, Hanin J. Progressive statistics for studies in sports medicine and exercise science. *Med Sci Sports Exerc*. 2009;41(1):3-12. doi:10.1249/MSS.0b013e31818cb278.

30. Bland JM, Altman DG. Statistical methods for assessing agreement between two methods of clinical measurement. *Int J Nurs Stud*. 2010;47(8):931-936. doi:10.1016/j.ijnurstu.2009.10.001.

31. Udofa AB, Ryan LJ, Weyand PG. Impact Forces During Running: Loaded Questions, Sensible Outcomes. In: *IEEE 13th International Conference on Wearable and Implantable Body Sensor Networks (BSN)*. ; 2016:371-376.

32. Vigh-Larsen JF, Dalgas U, Andersen TB. Position-Specific Acceleration and Deceleration Profiles in Elite Youth and Senior Soccer Players. *J Strength Cond Res*. 2018;32(4):1114-1122. doi:10.1519/JSC.0000000000001918.

33. Dalen T, Jørgen I, Gertjan E, Havard HG, Ulrik W. Player load, Acceleration, and Deceleration during 45 Competitive Matches of Elite Soccer. *J Strength Cond Res*. 2016;30(2):351-359.

34. Datson N, Drust B, Weston M, Gregson W. Repeated high-speed running in elite female soccer players during international competition. *Sci Med Footb*. 2018:1-7. doi:10.1080/24733938.2018.1508880.

35. Akenhead R, Hayes PR, Thompson KG, French D. Diminutions of acceleration and deceleration output during professional football match play. *J Sci Med Sport*. 2013;16(6):556-561. doi:10.1016/j.jsams.2012.12.005.

36. Kyröläinen H, Avela J, Komi P V. Changes in muscle activity with increasing running speed. *J Sports Sci*. 2005;23(10):1101-1109. doi:10.1080/02640410400021575.

37. Harper DJ, Kiely J. Damaging nature of decelerations: Do we adequately prepare players? *BMJ Open Sport Exerc Med*. 2018;4(e000379):1-3. doi:10.1136/bmjsem-2018-000379.

38. Roetenberg D, Luinge H, Slycke P. *Xsens MVN: Full 6DOF Human Motion Tracking Using Miniature Inertial Sensors*.; 2013. doi:10.1.1.569.9604.

39. Karatsidis A, Bellusci G, Schepers MH, de Zee M, Andersen MS, Veltink PH. Estimation of Ground Reaction Forces and Moments During Gait Using Only Inertial Motion Capture. *Sensors*. 2017;17(75):1-22. doi:10.3390/s17010075.

40. Jamkrajang P, Robinson MA, Limroongreungrat W, Vanrenterghem J. Can segmental model reductions quantify whole-body balance accurately during dynamic activities? *Gait Posture*. 2017;56(March):37-41. doi:10.1016/j.gaitpost.2017.04.036.

41. Perrott MA, Pizzari T, Cook J, McClelland JA. Comparison of lower limb and trunk kinematics between markerless and marker-based motion capture systems. *Gait Posture*. 2017;52:57-61. doi:10.1016/j.gaitpost.2016.10.020.

42. Abrams GD, Harris AHS, Andriacchi TP, Safran MR. Biomechanical analysis of three tennis serve types using a markerless system. *Br J Sports Med*. 2014;48(4):339-342. doi:10.1136/bjsports-2012-091371.

43. Grigg J, Haakonssen E, Rathbone E, Orr R, Keogh JWL. The validity and intra-tester reliability of markerless motion capture to analyse kinematics of the BMX Supercross gate start. *Sport Biomech*. 2018;17(3):383-401. doi:10.1080/14763141.2017.1353129.

44. Sperlich B, Düking P, Holmberg H-C. A SWOT Analysis of the Use and Potential Misuse of Implantable Monitoring Devices by Athletes. *Front Physiol*. 2017;8(629):1-3. doi:10.3389/fphys.2017.00629.

45. Wouda FJ, Giuberti M, Bellusci G, et al. Estimation of Vertical Ground Reaction Forces and Sagittal Knee Kinematics During Running Using Three Inertial Sensors. *Front Physiol*. 2018;9(March):1-14. doi:10.3389/fphys.2018.00218.

46. Johnson WR, Mian A, Donnelly CJ, Lloyd D, Alderson J. Predicting athlete ground reaction forces and moments from motion capture. *Med Biol Eng Comput*. 2018.

47. Pogson M, Verheul J, Robinson MA, Vanrenterghem J, Lisboa PJ. Estimating mechanical load in running activities: A neural network method to predict task- and step-specific ground reaction forces from trunk acceleration. *Under Rev*. 2018.

48. Johnson WR, Alderson J, Lloyd DG, Mian A. Predicting Athlete Ground Reaction Forces and Moments from Spatio-temporal Driven CNN Models. *IEEE Trans Biomed Eng*. 2018. doi:10.1109/TBME.2018.2854632.

49. Lee MK, Le NS, Fang AC, Koh MTH. Measurement of body segment parameters using dual energy X-ray absorptiometry and three-dimensional geometry: An application in gait analysis. *J Biomech*. 2009;42(3):217-222. doi:10.1016/j.jbiomech.2008.10.036.

50. Durkin JL, Dowling JJ, Andrews DM. The measurement of body segment inertial parameters using dual energy X-ray absorptiometry. *J Biomech*. 2002;35:1575-1580. doi:10.1016/S0021-9290(02)00227-0.

51. Camomilla V, Dumas R, Cappozzo A. Human movement analysis: The soft tissue artefact issue. *J Biomech*. 2017;62:1-4. doi:10.1016/j.jbiomech.2017.09.001.

52. Bezodis NE, Salo AIT, Trewartha G. Excessive fluctuations in knee joint moments during early stance in sprinting are caused by digital filtering procedures. *Gait Posture*. 2013;38:653-657.

doi:10.1016/j.gaitpost.2013.02.015.

53. Robertson DGE, Dowling JJ. Design and responses of Butterworth and critically damped digital filters. *J Electromyogr Kinesiol*. 2003;13(6):569-573. doi:10.1016/S1050-6411(03)00080-4.

**Figure captions**

**Figure 1** Root mean square errors (RMSE) for resultant GRF curves estimated from fifteen segmental accelerations. Inset: representative measured (black solid line) and estimated (red dashed line) GRF profiles are shown, together with RMSE values for all acceleration (n=166), deceleration (n=161), 90° cut (n=171), low- (n=157), moderate- (n=157) and high-speed running (n=141) trials.

**Figure 2** Root mean square errors (RMSE) for estimated resultant GRF curves for each task. Bars represent the percentage of trials (primary y-axis) within the very low (<1 $N\cdot kg^{-1}$), low (1-2 $N\cdot kg^{-1}$), moderate (2-3 $N\cdot kg^{-1}$), high (3-4 $N\cdot kg^{-1}$) or very high (>4 $N\cdot kg^{-1}$) error boundaries, and black dots represent the mean errors (secondary y-axis), for each given number of segments.

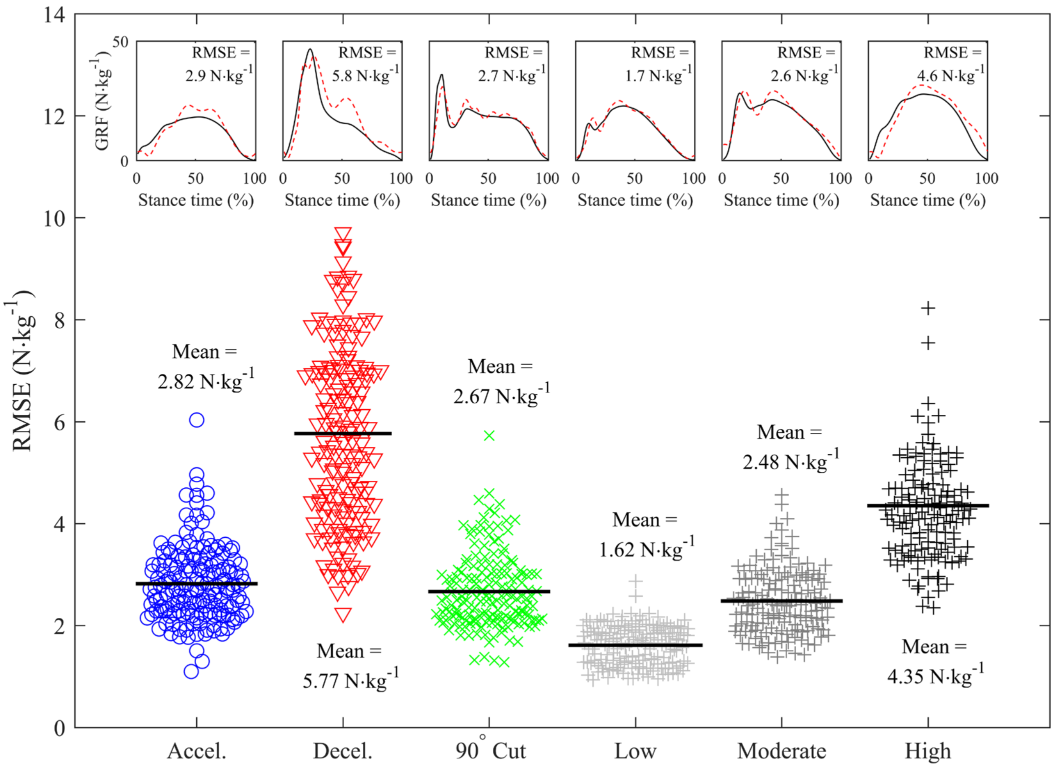
RMSE (N·kg-1)
Accel.
Decel.
90° Cut
Low
Moderate
High
Mean = 2.82 N·kg-1
Mean = 5.77 N·kg-1
Mean = 2.67 N·kg-1
Mean = 1.62 N·kg-1
Mean = 2.48 N·kg-1
Mean = 4.35 N·kg-1
GRF (N·kg-1)
Stance time (%)
RMSE = 2.9 N·kg-1
RMSE = 5.8 N·kg-1
RMSE = 2.7 N·kg-1
RMSE = 1.7 N·kg-1
RMSE = 2.6 N·kg-1
RMSE = 4.6 N·kg-1

485

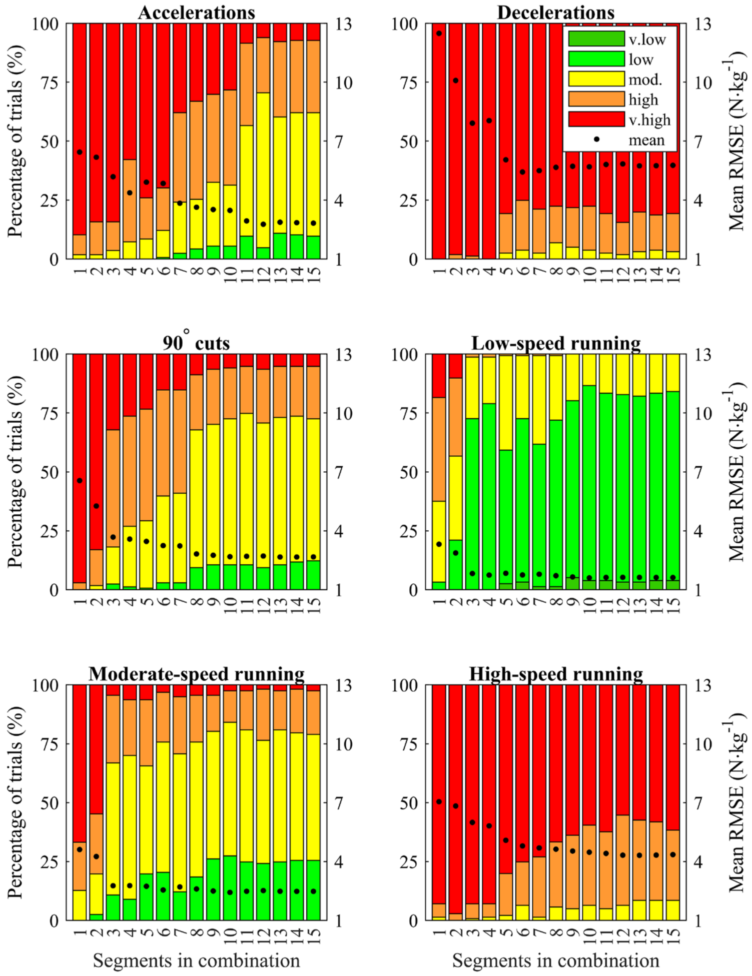

Accelerations
Decelerations
90° cuts
Low-speed running
Moderate-speed running
High-speed running
Percentage of trials (%)
Mean RMSE (N·kg⁻¹)
Segments in combination
v.low
low
mod.
high
v.high
mean

**Table 1** Estimated resultant ground reaction force curve and loading characteristics errors

| | **RMSE** | | **Impulse error** | | | **Impact peak error** | | | **Loading rate error** | | |
|---|---|---|---|---|---|---|---|---|---|---|---|
| | $N\cdot kg^{-1}$ | % | $N\cdot s\cdot kg^{-1}$ | % | $R^2$ | $N\cdot kg^{-1}$ | % | $R^2$ | $N\cdot kg^{-1}\cdot s^{-1}$ | % | $R^2$ |
| Accelerations (n=166) | 2.82 ±0.7 | 8.4 ±14 | 0.25 ±0.1 | 9.1 ±4 | 0.89 | 3.27 ±2.8 | 28.5 ±33 | 0.21 | 229 ±264 | 33.2 ±27 | 0.36 |
| Decelerations (n=161) | 5.77 ±1.8 | 6.1 ±8.8 | 0.26 ±0.1 | 11.1 ±6 | 0.94 | 7.68 ±5.5 | 15 ±9 | 0.73 | 380 ±404 | 20.1 ±16 | 0.49 |
| 90° cuts (n=171) | 2.67 ±0.7 | 3.3 ±4.1 | 0.21 ±0.1 | 3.8 ±2 | 0.98 | 3.33 ±2.9 | 9.8 ±8 | 0.75 | 234 ±210 | 24.5 ±18 | 0.60 |
| Constant speed running | | | | | | | | | | | |
| Low (2-3 $m\cdot s^{-1}$; n=157) | 1.62 ±0.4 | 1.8 ±2 | 0.09 ±0.06 | 2.3 ±2 | 0.96 | 2.22 ±2.3 | 13.8 ±22 | 0.64 | 173 ±101 | 33 ±13 | 0.42 |
| Moderate (4-5 $m\cdot s^{-1}$; n=157) | 2.48 ±0.6 | 3.1 ±5.7 | 0.16 ±0.1 | 4.6 ±2 | 0.93 | 1.96 ±1.5 | 9.2 ±8 | 0.85 | 281 ±174 | 34 ±14 | 0.53 |
| High (>6 $m\cdot s^{-1}$; n=141) | 4.35 ±1.3 | 6.4 ±7.6 | 0.26 ±0.2 | 10.4 ±12 | 0.77 | 3.52 ±3.5 | 11.9 ±13 | 0.56 | 661 ±419 | 42.8 ±21 | 0.12 |
| All tasks (n=953) | 3.26 ±1.7 | 4.8 ±8.3 | 0.20 ±0.1 | 6.8 ±7 | 0.99 | 4.00 ±4.1 | 13.1 ±15 | 0.88 | 323 ±326 | 29.3 ±19 | 0.68 |

Root mean square error (RMSE), impulse, impact peak and loading rate errors of the resultant GRF estimated from fifteen segmental accelerations, for different tasks. Values are means ± standard deviations and either absolute or relative errors compared to the measured resultant GRF. Regressions ($R^2$) were performed per task as well as for all trials combined.

## Appendix A: Marker attachment locations

Full-body kinematic data in this study were collected using a seventy-six retro-reflective marker set attached to anatomical landmarks of the body. The aim of this appendix is to clarify the attachment locations of segment defining and segment tracking markers (figure A.1). Markers for segment definition (of which some were also used for segment tracking; see figure A.1) were attached to the Calcaneus, lateral Calcaneus, first and fifth Metatarsus head, lateral/medial Malleolus, lateral/medial Epicondyle of the Femur, Femur greater Trochanter, anterior/posterior Superior Iliac Spine, Iliac Crest, Acromion, anterior/posterior head, shoulder, lateral/medial Epicondyle of the Humerus, Styloid process of the Radius and Ulna, lateral/medial Metacarpal head (all left and right), Cervical vertebrae 7, Thoracic vertebrae 8, and the Jugular notch and Xiphoid process of the Sternum. In addition, marker clusters for segment tracking were attached to the lateral sides of the shanks and thighs (four markers per cluster), as well as the forearms and upper arms (three markers per cluster).

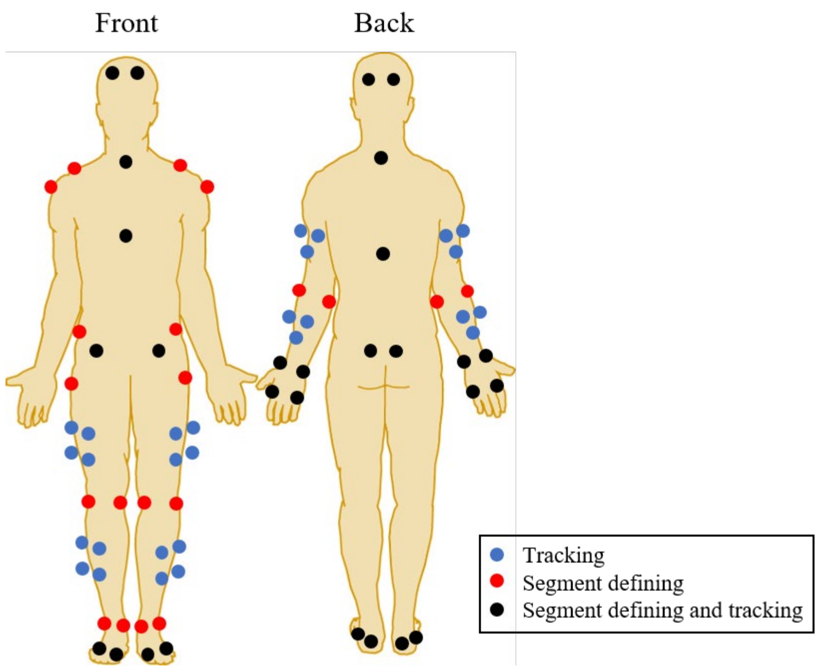


**Figure A.1** Attachment locations of segment tracking markers (blue), segment defining markers (red) and markers used for both (black).

## Appendix B: Marker trajectory filter cut-off frequencies

*Objective*

Segmental accelerations used to estimate ground reaction forces (GRFs) in this study were derived from motion capture-based marker trajectories. Accuracy of estimated GRF profiles is thus dependent on marker trajectory processing before calculating the segmental centre of mass (CoM) accelerations. The aim of this appendix was, therefore, to investigate what filter cut-off frequency lead to the most accurate resultant GRF estimates.

*Methods*

Kinematic and kinetic data for ten subjects (7 males and 3 females, age 24±5 yrs, height 176±8 cm, mass 72±9 kg) was used (see the methods section of the main paper for more detail on the data collection and processing). Marker trajectories were filtered with a $2^{nd}$ order Butterworth low-pass filter using four different cut-off frequencies (25 Hz, 20 Hz, 15 Hz and 10 Hz), while force data were filtered at 50 Hz. Visual screening of the data revealed relatively large trunk marker vibrations compared to the other markers, which was likely due to marker attachment to the shirt rather than the skin. Therefore, combinations of filter cut-off frequencies (20-15 Hz, 20-10 Hz and 15-10 Hz) were also examined, i.e. markers defining the trunk segment were filtered at a lower cut-off frequency than the other markers. Trunk defining markers that were filtered at a lower cut-off frequency were those attached to the left and right Iliac Crest and Acromion, Cervical vertebrae 7, Thoracic vertebrae 8, and the Jugular notch and Xiphoid process of the Sternum.

*Results*

Estimated GRF errors typically decreased for lower cut-off frequencies (table B.1). For higher frequencies (25 Hz, 20 Hz) the estimated GRF profiles included more oscillations compared to the lower cut-off frequencies (15 Hz, 10 Hz) (figure B.1). Consequently, RMSEs were lower across all tasks when marker data were filtered at 15 Hz, compared to 25 and 20 Hz. However, only for accelerations and constant speed running, errors were further reduced when a 10 Hz filter was applied, while over-smoothing of estimated GRF profiles resulted in the loss of important GRF characteristics (e.g. impact peak) for the other tasks (figure B.1 C, D, E). When a combination of two cut-off frequencies (20-15, 20-10 and 15-10 Hz) was used, however, RMSE values were further reduced. For most tasks separately, as well as all trials combined, a combination where the trunk was filtered at 10 Hz resulted in the most accurate GRF estimates (table B.1; figure B.1).

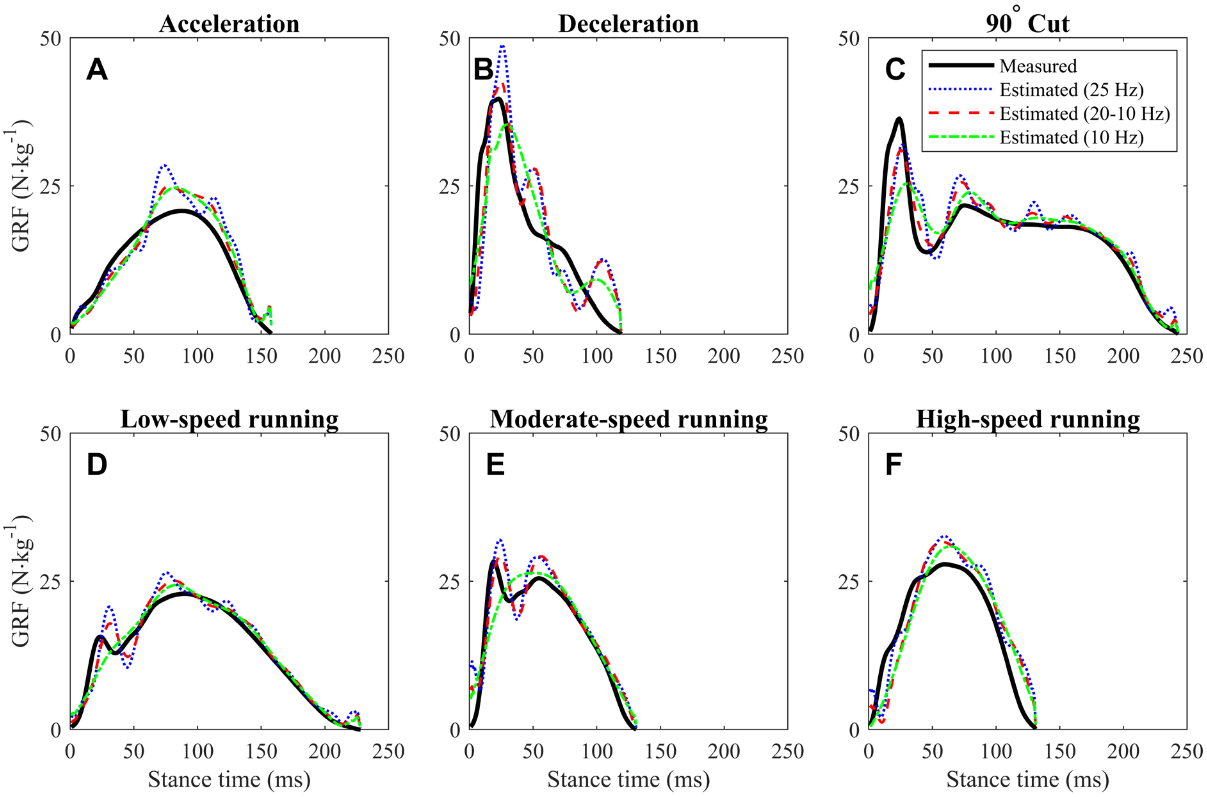


**Figure B.1** Representative examples of measured resultant ground reaction force (GRF; black solid line) profiles and resultant GRF estimated from marker trajectories filtered at 25 Hz (blue dotted line), 20-10 Hz (red dashed line) or 10 Hz (green dashed line), for each task.

**Table B.1** Marker trajectory filter cut-off frequency comparison

| | 25 Hz | 20 Hz | 20-15 Hz | 20-10 Hz | 15 Hz | 15-10 Hz | 10 Hz |
|---|---|---|---|---|---|---|---|
| Accelerations | 3.7±1 | 3.4±0.9 | 3.1±0.8 | 2.8±0.7 | 3±0.8 | 2.6±0.6 | 2.4±0.6 |
| Decelerations | 7.7±2.4 | 7.4±2.3 | 6.8±2 | 6±1.8 | 7.3±2.2 | 6.4±1.9 | 8±2.5 |
| 90° Cuts | 3.4±0.8 | 3.2±0.8 | 3±0.7 | 2.7±0.7 | 3.1±0.8 | 2.8±0.7 | 3.4±0.9 |
| Constant speed running | | | | | | | |
| Low (2-3 m·s$^{-1}$) | 2.3±0.6 | 2.1±0.6 | 1.9±0.5 | 1.7±0.4 | 1.9±0.5 | 1.6±0.4 | 1.7±0.5 |
| Moderate (4-5 m·s$^{-1}$) | 3.3±0.9 | 3.1±0.8 | 2.9±0.7 | 2.6±0.6 | 3±0.8 | 2.6±0.6 | 2.9±0.7 |
| High (>6 m·s$^{-1}$) | 5.4±1.3 | 5.1±1.3 | 4.8±1.2 | 4.4±1 | 4.9±1.2 | 4.4±1 | 4.7±1.3 |
| All tasks | 4.3±2.2 | 4.1±2.1 | 3.8±2 | 3.4±1.7 | 3.9±2.2 | 3.4±1.9 | 3.9±2.5 |

Root mean square errors (RMSE) for each (combination of) filter cut-off frequencies. Values are means ± standard deviation per task, as well as all tasks combined. The best cut-off frequency per task is highlighted in green shading.

*Conclusions*

Estimated resultant GRF profiles were more accurate across tasks when a combination of different cut-off frequencies was used for different markers. More specifically, the best results were obtained when marker trajectories were filtered at a 20 Hz cut-off frequency, with trunk defining markers filtered at 10 Hz. These cut-off frequencies were, therefore, used to filter marker trajectory data before further processing.

## Appendix C: Supplementary results

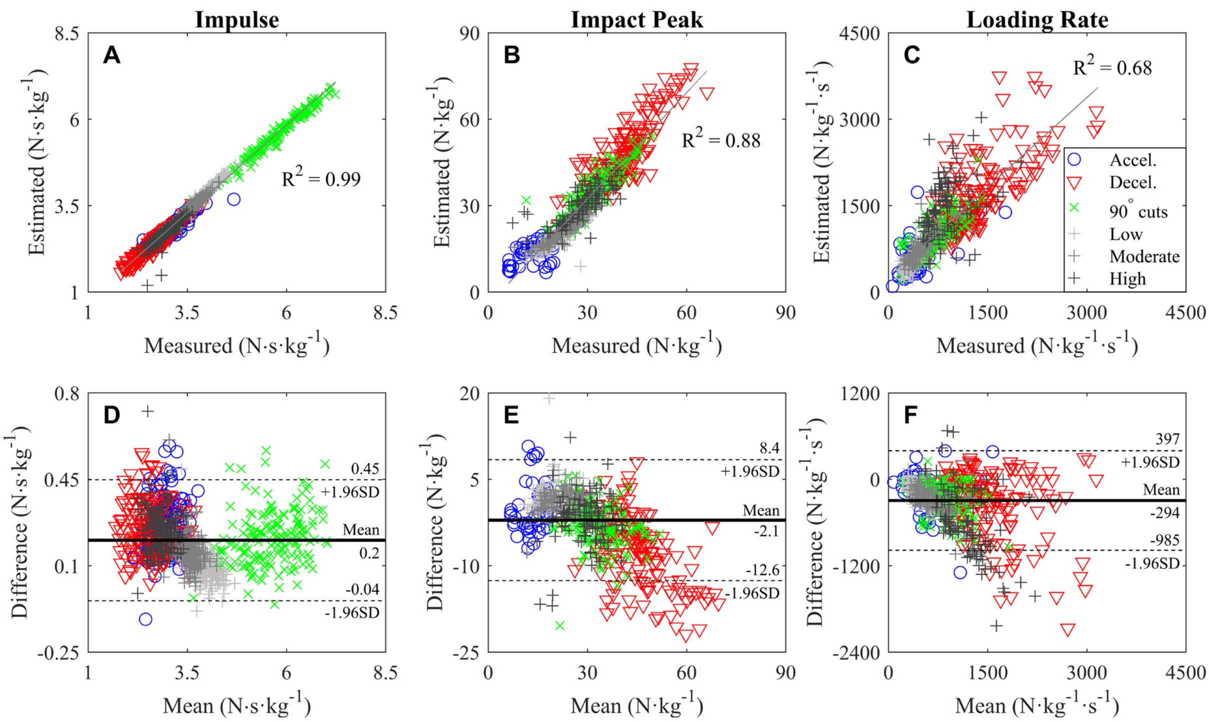


**Figure C.1** Regression (A-C) and Bland-Altman (D-F) plots between measured and estimated resultant GRF loading characteristics impulse, impact peak and loading rate.

**Table C.1** The best combinations of segments across all tasks for each given number of segments

| # | Segments in the combination | **RMSE ($N \cdot kg^{-1}$)** | |
|---|---|---|---|
| | | Mean | SD |
| 1 | Trunk | 6.76 | ±3.62 |
| 2 | Trunk + thigh | 5.91 | ±3.17 |
| 3 | Trunk + thighs | 4.54 | ±2.48 |
| 4 | Trunk + thighs + pelvis | 4.36 | ±2.47 |
| 5 | Trunk + thighs + pelvis + head | 4.00 | ±1.94 |
| 6 | Trunk + thighs + pelvis + shanks | 3.76 | ±1.81 |
| 7 | Trunk + thighs + shanks + head + upper arm | 3.61 | ±1.66 |
| 8 | Trunk + thighs + shanks + head + upper arm + forearm | 3.49 | ±1.73 |
| 9 | Trunk + thighs + shanks + head + upper arms + forearm | 3.42 | ±1.75 |
| 10 | Trunk + thighs + shanks + head + upper arms + forearms | 3.37 | ±1.74 |
| 11 | Trunk + thighs + shanks + head + upper arms + forearms + hand | 3.31 | ±1.73 |
| 12 | Trunk + thighs + shanks + head + upper arms + forearms + hand + foot | 3.28 | ±1.72 |
| 13 | Trunk + thighs + shanks + head + upper arms + forearms + hand + feet | 3.26 | ±1.71 |
| 14 | Trunk + thighs + shanks + head + upper arms + forearms + hands + feet | 3.26 | ±1.71 |
| 15 | Trunk + thighs + shanks + head + upper arms + forearms + hands + feet + pelvis | 3.26 | ±1.72 |

Best combinations of segments (i.e. with the lowest mean root mean square errors (RMSE) across subjects, tasks and trials) for each number of segments. If only one of two segments was included in a combination (e.g. thigh or foot rather than thighs or feet), this was the segment on the side of the support leg. SD = standard deviation.